Density-functional theory for spherical drops: II. Variable-range attractive forces



1995 J. Phys.: Condens. Matter 7 547

(http://iopscience.iop.org/0953-8984/7/3/010)

J. Phys.: Condens. Matter 7 (1995) 547–562. Printed in the UK

# Density-functional theory for spherical drops: II. Variable-range attractive forces

Ioannis A Hadjiagapiou
Solid State Physics Section, Department of Physics, University of Athens, Panepistimiopolis, Zografos GR 157-84, Athens, Greece

Received 11 July 1994, in final form 14 September 1994

**Abstract.** Using mean-field free-energy density functionals, we studied the structure of a liquid drop embedded in a vapour background of a one-component fluid, in the absence of an external field, using exponentially decaying fluid–fluid attractive interactions (characterized by an inverse range parameter $\lambda$) of the type employed by Sullivan. In Sullivan's original model and afterwards, $\lambda$ was specified by the arbitrary condition $\lambda d = 1$ ($d$ is the hard-sphere diameter). Now, this choice is relaxed and the potential is allowed to have variable inverse range parameter as well as attractive forces between fluid molecules; as a result, some of the interfacial quantities vary with $\lambda$ and some do not. Those influenced by $\lambda$ are the density profiles, principal tensors, surface tensions ($\gamma_{mech}$ and $\gamma_{therm}$) according to the mechanical and thermodynamic routes, the radii of the dividing surfaces and the homogeneous radius; while those not influenced by $\lambda$ are the pressure difference $\Delta p$ across the drop, the density $\rho(0)$ at the drop centre, the equimolar surface tension $\gamma_e$ and the existence of a homogeneous phase inside the drop; however large the drop may be, this behaviour of the drop depends only on the supersaturation.

## 1. Introduction

Several years ago Sullivan developed an elegant microscopic theory of wetting of a solid substrate by a bulk vapour phase, treating the solid as an external one-dimensional potential $V(z)$ acting on the atoms of the fluid and considering planar dividing surfaces [1]. In Sullivan's original model the attractive part $w(r)$ of the fluid–fluid interaction is a decaying exponential with an inverse range parameter $\lambda_F$ identical to that $\lambda_W$ of the solid–fluid attractive potential, which is also exponentially decaying, i.e. $\lambda_F = \lambda_W = \lambda$. As a result of this choice, the wetting of the solid substrate changes continuously from partial wetting to complete at some temperature $T_W$. This wetting transition is second-order, contrary to Cahn's phenomenological theory, predicting a first-order transition. In an attempt to resolve this discrepancy, Evans *et al* [2] and Teletzke *et al* [3] relaxed the condition of equal inverse range parameters and studied the corresponding generalized Sullivan model, concluding that the wetting transition can be first- or second-order depending on the ratio of the inverse range parameters and the strength of the solid–fluid interaction (see also [4]). Thus the choice $\lambda_F \neq \lambda_W$ yields significant changes in the wetting behaviour of the system. In addition, Sullivan's original model includes the arbitrary condition $\lambda d = 1$ (also used elsewhere [2, 5]), chosen to simplify the mathematical expressions. This choice obscures the possible influence of $\lambda$ on the interfacial properties of the system under consideration.

In an earlier communication [6], Sullivan's model was applied to a one-component system comprising a liquid drop and its bulk vapour in the absence of an external field. In this case, there was only one inverse range parameter, $\lambda_F \equiv \lambda$, associated with the fluid–fluid attractive interaction, chosen such that $\lambda d = 1$. However, this restriction is arbitrary,

0953-8984/95/030547+16$19.50  

so it can be relaxed, and $\lambda$ behaves as a degree of freedom, taking values in the domain $(0, \infty)$. The other degree of freedom is the temperature $T$ for the planar interface and the doublet $(T, \rho_{vs})$ for the spherical interface; $\rho_{vs}$ is the bulk vapour density. Relaxing this restriction, the attractive potential and forces acquire a variable range, because $\lambda^{-1}$ is a measure of the range of these forces, and $\lambda$ influences some of the interfacial quantities of the system (i.e. the density profile, principal tensors, surface tensions ($\gamma_{mech}$ and $\gamma_{therm}$) according to the mechanical and thermodynamic routes, the radii of the dividing surfaces and the homogeneous radius $R_{hom}$, which is the radius of the sphere, inside the drop, wherein the density remains constant) while some are constant with respect to $\lambda$ (the pressure difference $\Delta p$ across the drop, the density $\rho(0)$ at the drop centre and the equimolar surface tension $\gamma_e$). In addition, $\lambda$ does not influence the distribution of the fluid molecules inside the drop (interior phase), in that a large drop does not always encompass a homogeneous phase, this property depends only on the supersaturation.

In section 2 we outline, in brief, the mean-field theory (MFT) of the density profiles, pressure tensor and surface tensions for a planar and spherical interface, with $\lambda$ being a variable. Section 3 is devoted to the discussion of the numerical results, while in section 4, we discuss the results and compare them with the ones for $\lambda d = 1$ [6].

## 2. Theory

### *2.1. Density profile*

We consider the general grand potential functional for a one-component system (in the absence of an external field)

$$\Omega_V[\rho(r)] = \int_V \mathrm{d}r \left( f_h[\rho(r)] + \tfrac{1}{2}\rho(r) \int_V \rho(r') w(|r - r'|)\, \mathrm{d}r' - \mu\rho(r) \right) \tag{2.1}$$

where $\rho(r)$ is the average number density at point $r$, $\mu$ the bulk vapour chemical potential and $V$ the volume of the system. The repulsive force contribution to the Helmholtz free energy is treated in the local-density approximation in that $f_h[\rho(r)]$ is the Helmholtz free-energy density of a uniform hard-sphere fluid at density $\rho(r)$, while the attractive forces are treated in mean-field approximation so that $w(r)$ is the attractive part of the pairwise potential between two fluid molecules [5–8].

The equilibrium density $\rho(r)$ minimizes the functional (2.1) and, by setting $\delta\Omega[\rho(r)]/\delta\rho(r) = 0$, the Euler–Lagrange equation results:

$$\mu = \mu_h[\rho(r)] + \int_V w(|r - r'|)\rho(r')\, \mathrm{d}r' \tag{2.2}$$

where $\mu_h[\rho(r)] = \partial f_h[\rho(r)]/\partial\rho(r)$ is the hard-sphere chemical potential. When (2.2) is substituted into (2.1) the equilibrium grand potential $\Omega_V$ results. The solution to the integral equation (2.2), once $w(r)$ is known, yields the density profile for a given geometry of the system. However, (2.2) can be converted to a non-linear second-order differential equation by choosing properly the interaction potential, because in this case the calculations become less expensive and the numerical methods for the solution of differential equations are better developed [1]:

$$w(r) = -(\alpha\lambda^3/4\pi)\mathrm{e}^{-\lambda r}/\lambda r. \tag{2.3}$$

Here $\alpha$ is

$$\alpha = -\int_V w(r)\,\mathrm{d}r \tag{2.4}$$

and $\lambda$ is an inverse range parameter; the influence of $\lambda$ on the system was overlooked since $\lambda d$ was put equal to unity previously. This is an arbitrary choice, mainly to simplify the mathematical expressions and to make the calculations easier. In a way, this restriction on $\lambda$ obscures its influence on the behaviour of the system; so we consider that this choice (i.e. $\lambda d = 1$) is no longer valid and regard it as a continuous variable taking positive values.

For the calculations that follow, the Carnahan–Starling equation of state for hard spheres is adopted:

$$p_h(\rho) = \rho k_B T(1 + \eta + \eta^2 - \eta^3)/(1 - \eta)^3 \tag{2.5}$$

where $\eta = \pi\rho d^3/6$ is the packing fraction, $T$ the temperature and $k_B$ the Boltzmann constant. The configurational part of the hard-sphere chemical potential is given by

$$\mu_h(\rho) = k_B T[\ln\eta + (8\eta - 9\eta^2 + 3\eta^3)/(1 - \eta)^3)]. \tag{2.6}$$

The critical density $\rho_c$ and temperature $T_c$ of the above model are given by the equations [1]:

$$\rho_c d^3 = 0.249 \qquad \alpha/(k_B T_c d^3) = 11.102. \tag{2.7}$$

Initially we assume spherically symmetric solutions, $\rho(r) = \rho(r)$, to equation (2.2) and that the centre of the drop coincides with the origin of the coordinate axes. The integration in (2.2) over the polar angles $\theta$, $\phi$ can be done analytically:

$$\mu = \mu_h(u) - \frac{\alpha}{2u}\int_0^\infty u'\rho(u')(\mathrm{e}^{-|u-u'|} - \mathrm{e}^{-|u+u'|})\,\mathrm{d}u' \tag{2.8}$$

where $u = \lambda r$, the dimensionless radial distance from the centre of the drop. By differentiating twice the integral equation (2.8) with respect to $u$, we obtain

$$\frac{\mathrm{d}^2\mu_h(u)}{\mathrm{d}u^2} + \frac{2}{u}\frac{\mathrm{d}\mu_h(u)}{\mathrm{d}u} - \mu_h(u) + \mu = -\alpha\rho(u) \tag{2.9a}$$

which is identical to that found in [6].

In the system under consideration (either with spherical or planar interface) $\lambda$ is considered as an additional independent variable. The other independent variable is $r$, so $u$ cannot be treated, any longer, as the independent variable in (2.9*a*), since it contains both $\lambda$ and $r$. Instead, another spatial variable is introduced by the transformation $u = \lambda r = (\lambda d)(r/d) = \Lambda v$, so that (2.9*a*) is transformed into

$$\frac{\mathrm{d}^2\mu_h(v)}{\mathrm{d}v^2} + \frac{2}{v}\frac{\mathrm{d}\mu_h(v)}{\mathrm{d}v^2} + [\mu - \mu_h(v)]\Lambda^2 = -\alpha\Lambda^2\rho(v) \tag{2.9b}$$

and $\lambda$ is now separated from $r$. The new reduced radial distance is now the variable $v = r/d$ and $\Lambda = \lambda d$ is the reduced inverse range parameter.

The differential equation (2.9*b*) is supplemented by the proper boundary conditions, which are identical to those in [6], i.e.

$$\mu_h'(0) = 0 \qquad \mu_h(\infty) = \mu_h^v \qquad \mu_h'(\infty) = 0 \tag{2.10}$$

so that the solution to (2.9*b*) is bounded; the prime denotes differentiation with respect to distance.

Considering as dependent variable the packing fraction $\eta(v)$ instead of $\mu_h(v)$, on substituting the Carnahan–Starling relation (2.6) in (2.9*b*) it yields, for $u \neq 0$,

$$\eta''(v) = -(2/v)\eta'(v) - B_1(\eta)\eta'^2(v) - \Lambda^2[B_2(\eta) + B_3(\eta)\eta(v)] \tag{2.11}$$

subject to the boundary conditions

$$\eta'(0) = 0 \qquad \eta(\infty) = \eta_v \qquad \eta'(\infty) = 0 \tag{2.12}$$

where

$$A_1 = \frac{\partial(\beta\mu_h)}{\partial\eta} = \frac{1}{\eta} + \frac{8-2\eta}{(1-\eta)^4} \qquad A_2 = \frac{\partial A_1}{\partial\eta} = -\frac{1}{\eta^2} + \frac{30-6\eta}{(1-\eta)^5} \tag{2.13a}$$

$$B_1(\eta) = \frac{A_2(\eta)}{A_1(\eta)} \qquad B_2(\eta) = \frac{\beta\mu - \beta\mu_h(\eta)}{A_1(\eta)} \qquad B_3(\eta) = \frac{6\alpha\beta}{\pi A_1(\eta)} \tag{2.13b}$$

and $\beta = (k_B T)^{-1}$.

In the neighbourhood of the drop's origin, the solution is expanded in a power series about $v = 0$ (see [6]):

$$\eta(v) = q + (v^2/2!)\eta^{(2)}(0) + (v^4/4!)\eta^{(4)}(0) \qquad \text{as } v \to 0 \tag{2.14}$$

where $q \equiv \eta(0)$ and the derivatives are

$$\eta^{(2)}(0) = -\tfrac{1}{3}[B_2(q) + qB_3(q)] \tag{2.15a}$$

$$\eta^{(4)}(0) = -\frac{3}{5}\left\{2B_1(q)[\eta^{(2)}(0)]^2 + \eta^{(2)}(0)\left[\left(\frac{dB_2(\eta)}{d\eta}\right)_{v=0} + q\left(\frac{dB_3(\eta)}{d\eta}\right)_{v=0} + B_3(q)\right]\right\}. \tag{2.15b}$$

For the subsequent calculations, all the quantities and equations are transformed to the dimensionless 'reduced' units:

$$\begin{aligned} &\mu^* = \mu/(k_B T) \qquad p^* = d^3 p/(k_B T) \qquad T^* = T/T_c \\ &\gamma^* = d^2\gamma/(k_B T) \qquad \rho^* = \rho d^3 \qquad \alpha^* = \alpha/(k_B T d^3) = 11.102/T^*. \end{aligned} \tag{2.16}$$

Thus

$$\begin{aligned} \mu^*(\rho^*, T^*) &= \mu_h^*(\rho^*, T^*) - \alpha^*\rho^* \\ p^*(\rho^*, T^*) &= p_h^*(\rho^*, T^*) - \alpha^*\rho^{*2}/2. \end{aligned} \tag{2.17}$$

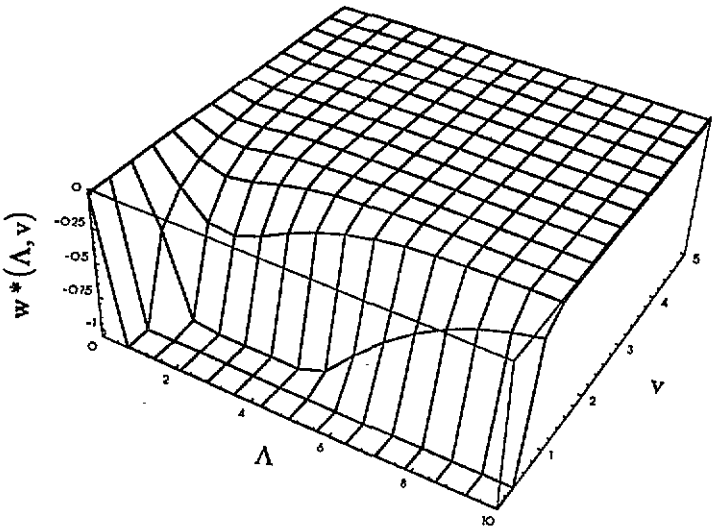


**Figure 1.** Attractive potential $w^*(\Lambda, v) \equiv [4\pi/(11.102k_BT_c)]w(\Lambda, v)$ versus $(\Lambda, v)$.

Although the asterisks, for simplicity in the expressions, will be suppressed, all the results will be with respect to the above dimensionless variables (2.16). The interaction potential (2.3) in terms of $\Lambda$ and $v$ can be written as

$$w(\Lambda, v) = -(11.102k_BT_c/4\pi)\Lambda^3 \exp(-\Lambda v)/\Lambda v \tag{2.18}$$

which is now an explicit function of the two variables $\Lambda$ and $v$; its graph appears in figure 1. The attractive potential $w(\Lambda, v)$ as a function of $\Lambda$ (constant distance $v$) has a minimum given by the relation $\Lambda v = 2$, while for constant $\Lambda$ it is an increasing function of the distance, tending to zero as $v$ diverges.

According to Gibbs phase rule, a one-component two-phase system has only one degree of freedom, and as such the temperature $T$ is chosen here. In the present case, the system with a planar interface has an additional degree of freedom, namely $\Lambda$. The system with a spherical interface possesses two extra degrees of freedom, the bulk vapour density $\rho_{vs}$ (varying in the interval $(\rho_{vc}, \rho_{vsp})$, where $\rho_{vc}$ is the vapour density for a planar dividing surface at the same temperature $T$ and $\rho_{vsp}$ the corresponding spinodal density) and the reduced inverse range parameter $\Lambda$; this is not the only possible choice. For a given value of $T$ and $\rho_{vs}$ one can find an infinite number of drops that correspond to the possible values of $\Lambda$; all these drops have identical bulk vapour density and density at the drop's origin $\rho(0)$ that is identical to the one for $\Lambda = 1$ [6].

The variation of $\Lambda$ also influences the behaviour of the liquid–vapour system with a planar dividing surface. In this case the governing equation resulting from (2.2) is

$$\mu = \mu_h(z_1) - \frac{\alpha}{2}\int_0^\infty z_1'\rho(z_1')(e^{-|z_1-z_1'|} - e^{-|z_1+z_1'|})\,dz_1' \tag{2.19}$$

where $z_1 = \lambda z$ and the dividing surface coincides with the $xy$ plane. When (2.19) is differentiated twice with respect to $z_1$, it yields

$$d^2\mu_h(z_1)/dz_1^2 - \mu_h(z_1) + \mu = -\alpha\rho(z_1) \tag{2.20}$$

(see [1]). The solution to (2.20) has to obey the asymptotic behaviour

$$\mu_h(\infty) = \mu_h^v \qquad \mu_h'(\infty) = 0. \tag{2.21}$$

The differential equation (2.20) can be integrated once, yielding

$$d\mu_h(z_1)/dz_1 = -\{[\mu_h(z_1) - \mu]^2 - 2\alpha[p_h(z_1) - p]\}^{1/2} \tag{2.22a}$$

on recalling (2.21), the minus sign in front of the square root is necessary because the bulk phase is vapour and $p$ is the bulk pressure [1].

As previously, the independent variable $z_1$ in (2.22*a*) is replaced so that the $\Lambda$ dependence is separated from the $z$ dependence. This is achieved through the transformation $z_1 = \lambda z = (\lambda d)(z/d) = \Lambda\zeta$ and (2.22*a*) becomes

$$d\mu_h(\zeta)/d\zeta = -\Lambda\{[\mu_h(\zeta) - \mu]^2 - 2\alpha[p_h(\zeta) - p]\}^{1/2}. \tag{2.22b}$$

In (2.22*b*) we consider again as dependent variable the packing fraction $\eta(\zeta)$ instead of $\mu_h(\zeta)$. Thus on recalling the Carnahan–Starling relation (2.6), (2.22*b*) becomes

$$d\eta(\zeta)/d\zeta = -[\Lambda/A_1(\eta)]\{[\mu_h(\eta) - \mu]^2 - 2\alpha[p_h(\eta) - p]\}^{1/2} \tag{2.23}$$

where $A_1(\eta)$ is given by (2.13*a*).

### 2.2. *Pressure tensor and surface tension*

The system under consideration (with either a spherical or planar dividing surface) consists of, at least, one homogeneous phase and one inhomogeneous. In the former case, the two pressure tensor components (normal $p_N$ and transverse $p_T$) are equal to each other and identical to the pressure of the respective phase. In the latter case, these components are unequal and vary with distance, in general. The only condition satisfied by the pressure tensor $p(r)$ is the vanishing of its divergence owing to the mechanical equilibrium of the system under consideration, i.e.

$$\nabla \cdot p(r) = 0 \tag{2.24}$$

in the absence of an external field [6, 7].

The pressure tensor for a spherical interface consists of the normal $p_N(r)$ and transverse $p_T(r)$ components, which are related by the equation

$$p_N'(r) = (2/r)[p_T(r) - p_N(r)] \tag{2.25}$$

a result of (2.24) for the respective geometry. Integrating (2.25) from inside to outside yields

$$p_N(0) - p_N(\infty) = 2\int_0^\infty \frac{p_N(r) - p_T(r)}{r}\,dr. \tag{2.26}$$

The left-hand side can be considered as one of the possible definitions of the pressure difference $\Delta p$ across the drop. Equation (2.25) can also be regarded as a differential equation for $p_N(r)$, once $p_T(r)$ is known, i.e.

$$\tfrac{1}{2}r\,dp_N(r)/dr + p_N(r) = p_T(r) \tag{2.27a}$$

so that

$$p_N(r) = \frac{2}{r^2}\int_0^r p_T(r_1) r_1 \, dr_1. \tag{2.27b}$$

The $p_T(r)$ component can be identified with minus the grand potential free-energy density, i.e.

$$p_T(r) = -\omega[\rho_0(r)] \tag{2.28}$$

where $\rho_0(r)$ is the equilibrium density. On substituting (2.2) into (2.1) we get

$$p_T(r) = p_h[\rho_0(r)] + \tfrac{1}{2}\rho_0(r)\int_V \rho_0(r_1) w(|r - r_1|)\, dr_1. \tag{2.29}$$

Multiplying (2.9*b*) by $\mu_h'(v)$ and integrating from a point deep inside the drop to one in the bulk vapour phase yields

$$[\mu_h'^2(\rho) - \Lambda^2(\mu_h(\rho)-\mu)^2 + 2\alpha\Lambda^2 p_h(\rho)]_{\text{outside}} - [\mu_h'^2(\rho) - \Lambda^2(\mu_h(\rho)-\mu)^2 + 2\alpha\Lambda^2 p_h(\rho)]_{\text{inside}}$$
$$= -\int_{\text{inside}}^{\text{outside}} \frac{4}{v}\mu_h'^2(v)\, dv. \tag{2.30a}$$

The quantity in the bracket equals $2\alpha\Lambda^2 p(\rho)$ since $\mu_h'(v)$ vanishes at both ends and (2.30*a*) can be written

$$p_{\text{inside}} - p_{\text{outside}} = \int_{\text{inside}}^{\text{outside}} \frac{2}{\alpha\Lambda^2 v}\mu_h'^2(v)\, dv \tag{2.30b}$$

which is a generalization of the Young–Laplace equation. Its left-hand side can be considered as another definition of the pressure difference $\Delta p$ that monitors the variation of the density profile in the interfacial region and inside the drop (for a small one).

Another important quantity is the surface tension, which depends on the position of the dividing surface, in general. It is defined as the grand potential per unit surface area and, in the reduced units (2.16), is given by (see [6])

$$\gamma(R_\gamma; \Delta_p) = \frac{1}{3\alpha\Lambda R_\gamma^2}\int_0^\infty [v\mu_h'(v)]^2\, dv + \tfrac{1}{3}\Lambda R_\gamma \Delta p \tag{2.31}$$

where $R_\gamma$ is the radius of the dividing surface. For the radius $R_\gamma$ there are various alternative choices due to the different dividing surfaces. One such choice is the radius $R_s$ of the surface of tension, given by

$$R_s^3 = \frac{2}{\alpha\Lambda^2\Delta p}\int_0^\infty [v\mu_h'(v)]^2\, dv \tag{2.32a}$$

for which the curvature term in the Helmholtz free energy vanishes and the Young–Laplace equation retains its form [7]

$$\Delta p = 2\gamma(R_s)/R_s. \tag{2.32b}$$

Another choice for $R_\gamma$ is the radius $R_e$ of the equimolar dividing surface, given by the equation [7]

$$R_e^3 = \frac{1}{\rho_{vs} - \rho_{Ls}}\int_0^\infty v^3 \frac{d\rho(v)}{dv}\, dv. \tag{2.32c}$$

The mechanical route to the surface tension is defined through the relations (2.32*a, b*), while the thermodynamic route is defined through (2.32*b, c*) and

$$R_s = [3\gamma_\infty - (9\gamma_\infty^2 - 4\gamma_\infty R_e \Delta p)^{1/2}]/\Delta p \tag{2.32d}$$

see [6, 7].

## 3. Results

### 3.1. Density profiles

The differential equation (2.11) with the boundary conditions (2.12) was solved for various values of the two independent variables $\eta_{vs}$ and $\Lambda$ at a fixed reduced temperature $T^* = 0.8$ used also in [6]. The variable $\eta_{vs}$ assumes values within the interval $(\eta_{vc}, \eta_{vsp})$, where $\eta_{vc} = 0.021\,718\,09$ is the coexisting vapour packing fraction and $\eta_{vsp} = 0.061\,099\,63$ the corresponding spinodal packing fraction.

Let $R_T^*(\Lambda)$ be the reduced smallest distance from the centre of the drop where the density $\rho(r, \Lambda)$ assumes its bulk value $\rho_{vs}$. It was found in the numerical calculations that

$$R_T^*(\Lambda) = R_T^*(\Lambda = 1)/\Lambda \tag{3.1a}$$

resulting from the more general expression

$$R_T^*(\Lambda_1)/R_T^*(\Lambda_2) = \Lambda_2/\Lambda_1. \tag{3.1b}$$

So, instead of specifying $\Lambda$, $R_T^*(\Lambda)$ is given a value and $\Lambda$ is calculated from (3.1*a*) once $R_T^*(\Lambda = 1)$ is known. The chosen values for $R_T^*(\Lambda)$ were 50, 40, 30, 20, 10 and $R_T^*(\Lambda = 1)$. Equation (2.11) was solved for $\rho_{vs} = 0.05$, 0.075 and 0.1. Their plots appear in figure 2 and each individual density profile† in any plot is labelled by the corresponding $\Lambda$. The density profile for $\rho_{vs} = 0.05$ (small supersaturation) is characterized by the presence of a homogeneous phase inside the drop, evidenced by the straight line on the left-hand side of the profile, even for the smallest drop $R_T^*(\Lambda) = 10$ ($R_{hom}$ is non-vanishing). However, for the other two densities ($\rho_{vs} = 0.075$ and 0.1, high supersaturation) the extent of the homogeneous phase inside the drop is hardly perceptible even for the largest drop $R_T^*(\Lambda) = 50$, i.e. the behaviour of the density profiles in these cases is nearly identical to that for $\Lambda = 1$, so $R_{hom}$ is now negligible. This behaviour was also observed for very large radii, $R_T^*(\Lambda) = 100$, 500, 1000 and 1500, for $\rho_{vs} = 0.05$ and 0.1 (figure 3). These results indicate that a large drop, which may encompass a homogeneous phase (a necessary requirement of Laplacian thermodynamics) for a given bulk vapour density $\rho_{vs}$ (small supersaturation), does not always do so for a larger $\rho_{vs}$ value. The existence or not of a homogeneous phase inside a drop is independent of $\Lambda$ and depends only on the supersaturation, as in the case $\Lambda = 1$. Thus, although $\Lambda$ is a variable, the potential (2.3) cannot affect the structure of the system and the attractive forces behave as a uniform background potential. The hard-sphere potential still dominates the structure; their only effect is either to spread (that is, increase the extent of) or to contract the corresponding density profile for $\Lambda = 1$ [6], to accommodate the particles of the interior phase into the available space, but without changing the corresponding structure. For the radii $R_T^*(\Lambda)$ under consideration, the interfaces for $\rho_{vs} = 0.05$ separate two homogeneous phases, while for $\rho_{vs} = 0.075$ and $\rho_{vs} = 0.1$ the respective interfaces separate two phases that are either *inhomogeneous* or *negligibly homogeneous* ($R_{hom}$ *negligible*). This behaviour of the density profiles, for a specified $\rho_{vs}$, inside a drop is brought out by figure 4, where $R_{hom}$ is plotted. For small $\Lambda$ (or equivalently, large drops) only for the smaller $\rho_{vs} = 0.05$ is $R_{hom}$ significant and the corresponding drops contain a homogeneous 'bulk' phase.

As the supersaturation is lowered, the bulk vapour density $\rho_{vs}$ tends towards the planar interface density $\rho_{vs} = 0.041\,478\,49$ at the same reduced temperature $T^* = 0.8$; the

† *Remark.* The density profiles in figures 2 and 3 should tend smoothly to the respective bulk value but this was not achieved as satisfactorily as in figure 6 owing to computational problems in (2.11).

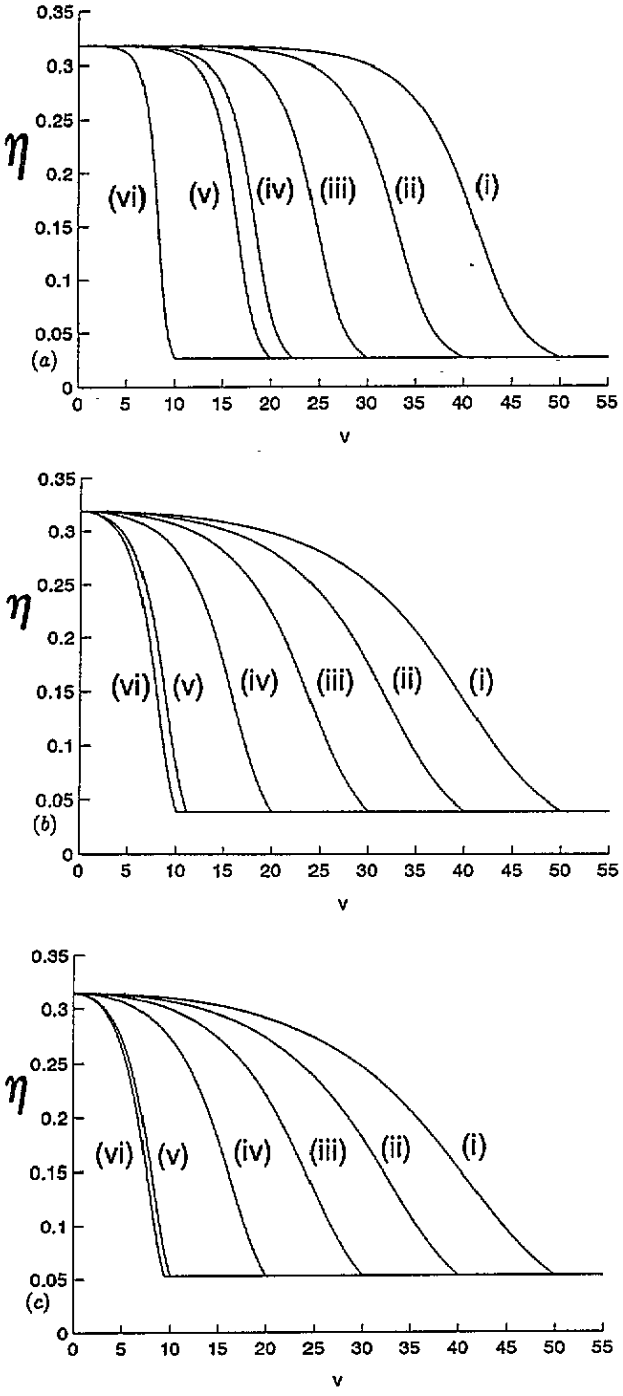


**Figure 2.** (*a*) Packing fraction $\eta(v, \Lambda)$ for $\rho_{vs} = 0.05$ versus reduced radial distance $v$ labelled by $\Lambda$: (i) 0.4459, (ii) 0.557 38, (iii) 0.743 17, (iv) 1, (v) 1.114 76, (vi) 2.229 52. (*b*) Packing fraction $\eta(v, \Lambda)$ for $\rho_{vs} = 0.075$ versus reduced radial distance $v$ labelled by $\Lambda$: (i) 0.222 18, (ii) 0.2777, (iii) 0.370 31, (iv) 0.555 46, (v) 1, (vi) 1.1109. (*c*) Packing fraction $\eta(v, \Lambda)$ for $\rho_{vs} = 0.1$ versus reduced radial distance $v$ labelled by $\Lambda$: (i) 0.187 86, (ii) 0.234 83, (iii) 0.313 11, (iv) 0.469 66, (v) 0.939 32, (vi) 1.

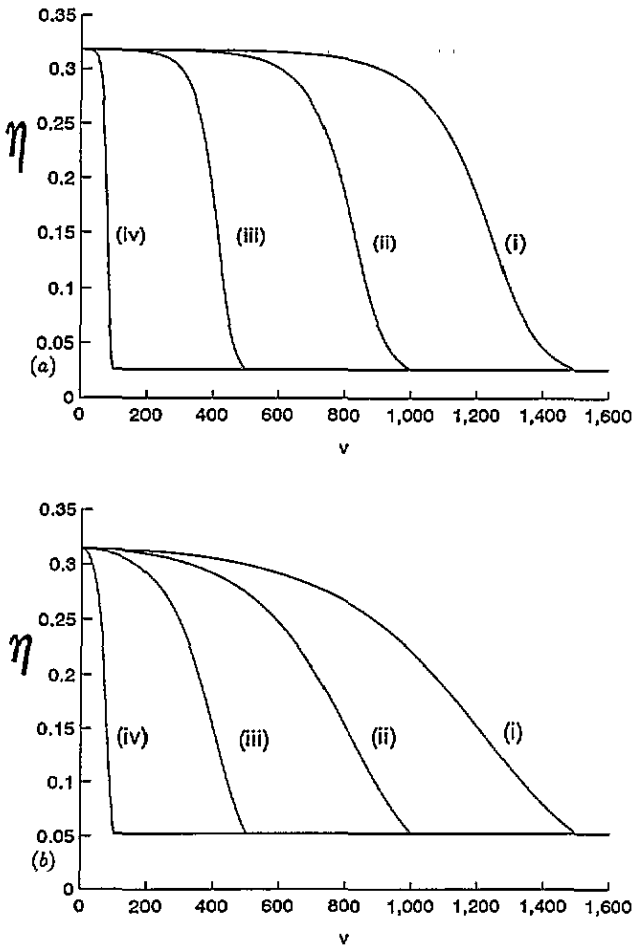


**Figure 3.** (*a*) Packing fraction $\eta(v, \Lambda)$ for $\rho_{vs} = 0.05$ versus radial distance $v$ for various $R_T^*(\Lambda)$ values: (i) 1500, (ii) 1000, (iii) 500, (iv) 100. (*b*) Packing fraction $\eta(v, \Lambda)$ for $\rho_{vs} = 0.1$ versus reduced radial distance $v$ for various $R_T^*(\Lambda)$ values: (i) 1500, (ii) 1000, (iii) 500, (iv) 100.

governing equation is (2.23), which also depends on $\Lambda$. In this case, the system is not finite but extends from $-\infty$ to $+\infty$; it behaves as a very large drop corresponding to the density $\rho_{vc}$. This behaviour depends strongly on $\Lambda$, in the sense that the smaller the $\Lambda$ the wider is the interfacial region and the longer is the distance from the origin of the axes, the density $\rho(\zeta, \Lambda)$ attains its bulk value $\rho_{vc}$, because the attractive forces are now of longer range. The existence of the homogeneous phase in the left-hand part of the density profile (liquid phase with density $\rho_{Lc} = 0.586731\,31$) is now more evident (see figure 5).

### *3.2. Pressure tensor and surface tension*

After the calculation of the density profile, all the other interfacial quantities can be evaluated. Either system under consideration (the one with spherical and the other with planar interface) possesses a particular symmetry that is also reflected in the corresponding pressure tensor $p(r)$, which, in both cases, consists of the two principal components $p_N(r)$ and $p_T(r)$. First, we examine the system with spherical symmetry. Both components $p_N(r)$

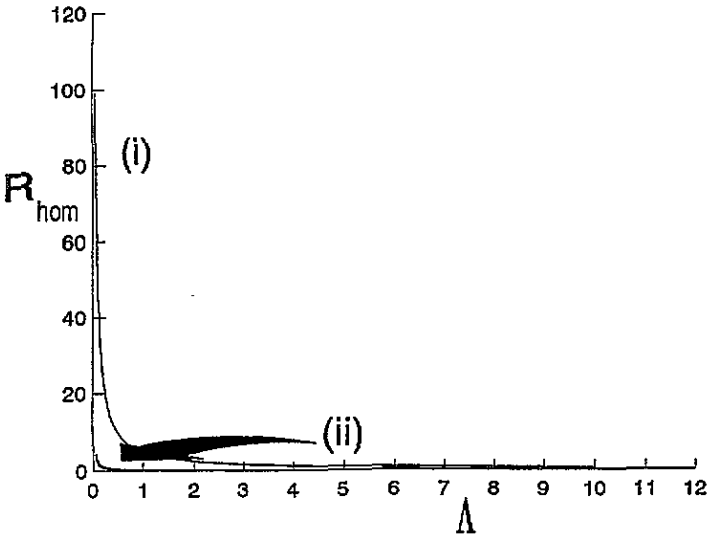


**Figure 4.** Radius $R_{hom}$ of the homogeneous-phase sphere versus $\Lambda$: (i) $\rho_{vs} = 0.05$, (ii) $\rho_{vs} = 0.075$, 0.1.

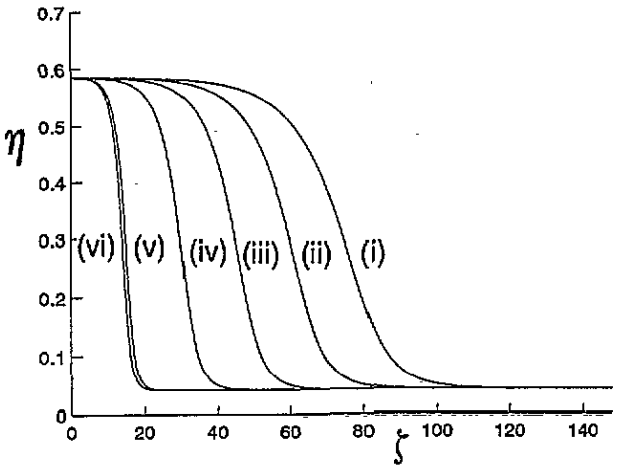


**Figure 5.** Packing fraction $\eta(v, \Lambda)$ for the flat interface (with density $\rho_{vc}$) at the same reduced temperature $T^* = 0.8$ versus reduced distance $\zeta$ for various $\Lambda$: (i) 0.187 86, (ii) 0.234 83, (iii) 0.313 11, (iv) 0.469 66, (v) 0.939 32, (vi) 1.

and $p_T(r)$ depend only on the radial distance $r$ from the origin of the drop and are given by (2.27*b*) and (2.29), respectively. For a given $\rho_{vs}$, regardless of $\Lambda$, they vary significantly within the interfacial region; but for $v \geqslant R_T^*(\Lambda)$ they join smoothly to their common value, coinciding with the bulk vapour pressure $p_v$ ($p_T(\infty) = p_N(\infty) = p_v$); also both coincide at $v = 0$ (figure 6). We also have the same situation as in the density profiles: for the drops with $\rho_{vs} = 0.05$ (small supersaturation), both components possess a plateau, reflecting the homogeneous phase existing inside the drop, which does not happen for the other two drops with $\rho_{vs} = 0.075$ and 0.1. For a specific $\rho_{vs}$ and its associated $\Lambda$ values, the profiles of

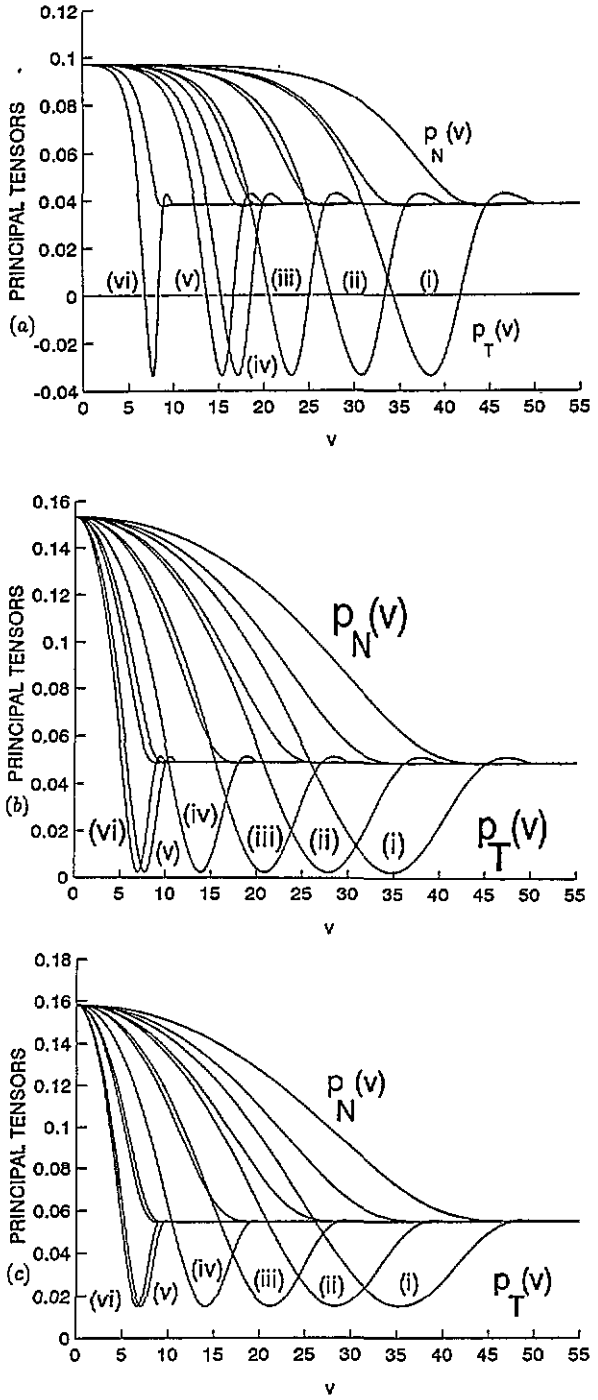


**Figure 6.** (*a*) Pressure tensor components for $\rho_{vs} = 0.05$ versus radial distance $v$ for various $\Lambda$: (i) 0.4459, (ii) 0.557 38, (iii) 0.743 17, (iv) 1, (v) 1.114 76, (vi) 2.229 52. (*b*) Pressure tensor components for $\rho_{vs} = 0.075$ versus radial distance $v$ for various $\Lambda$: (i) 0.222 18, (ii) 0.2777, (iii) 0.370 31, (iv) 0.555 46, (v) 1, (vi) 1.1109. (*c*) Pressure tensor components for $\rho_{vs} = 0.1$ versus radial distance $v$ for various $\Lambda$: (i) 0.187 86, (ii) 0.234 83, (iii) 0.313 11, (iv) 0.469 66, (v) 0.939 32, (vi) 1.

$p_N(r)$ and $p_T(r)$ are similar to those for $\Lambda = 1$, except that these are either spread if $\Lambda < 1$ or contracted if $\Lambda > 1$; also all the plots have the same minimum value occurring at different radial distances. For all the profiles the interface is initially under tension ($p_N(r) > p_T(r)$) while for larger distances it is under compression ($p_N(r) < p_T(r)$) only for $\rho_{vs} = 0.05$.

For the planar interface, $p_N(\zeta)$ is always constant, even in the interfacial region, and equal to the bulk vapour pressure, $p_N(\zeta) = p(\rho_{vc}) \equiv p_{flat}$ for all $\zeta$ and $\Lambda$ values. While $p_T(\zeta)$ varies with distance according to (2.29), it is mainly smaller than $p_N(\zeta)$ for all $\Lambda$ values, but becomes greater only in a small region on the vapour side of the profile before they join smoothly towards $p_{flat}$ (figure 7).

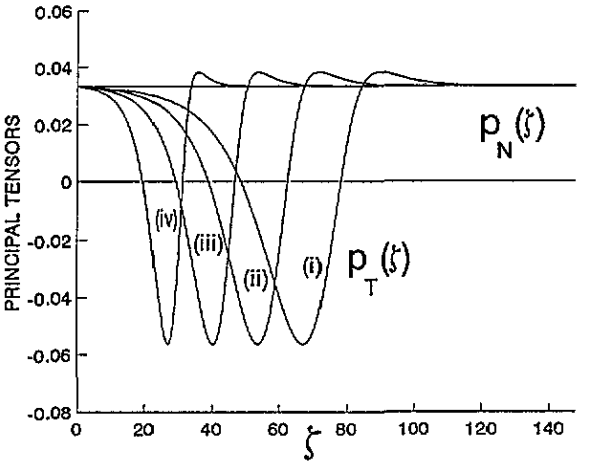


**Figure 7.** Flat interface pressure tensor components at the same reduced temperature $T^* = 0.8$ versus $\zeta$ for various $\Lambda$: (i) 0.187 86, (ii) 0.234 83, (iii) 0.313 11, (iv) 0.469 66. The straight line is $p_N(\zeta) = p_{flat}$.

For a spherical interface, the pressure difference $\Delta p$ is an ill-defined quantity (this does not happen for a planar interface); as a result, this behaviour affects the surface tension (2.31) and the radii (2.32*a*, *d*), since both depend explicitly on $\Delta p$ and $\Lambda$ (see [6]). For the numerical calculations, $\Delta p$ was calculated from (2.30*b*); although this expression depends explicitly on $\Lambda$, the numerical result was not sensitive to $\Lambda$ and thus $\Delta p$ is a constant for a given $\rho_{vs}$ and equal to that for $\Lambda = 1$ [6]. For the bulk vapour densities under consideration ($\rho_{vs} = 0.05$, 0.075 and 0.1) the corresponding surface tensions $\gamma_s$ according to the mechanical route and the surface tension $\gamma_{flat}$ for the flat interface decrease as $\Lambda$ increases. They join smoothly at about $\Lambda \simeq 8$, tending to zero as $\Lambda \to \infty$, and they seem to diverge as $\Lambda \to 0$ (figure 8(*a*)). For $\Lambda < 0.4$ and $\Lambda > 8$ they vary slowly and their difference is perceptible only in the interval $0.6 < \Lambda < 3$. In addition to $\gamma_s$, for density $\rho_{vs} = 0.05$ the surface tension $\gamma_{therm}$ according to the thermodynamic route and the equimolar $\gamma_e$ were calculated (see figure 8(*b*)); $\gamma_{therm}$ decreases as $\Lambda$ increases and is always below $\gamma_s$, while $\gamma_e$ is constant with respect to $\Lambda$, contrary to what one would expect. This behaviour of $\gamma_e$ is a significant drawback, for it cannot be considered as a measure of the surface tension; $\gamma_s$ and $\gamma_{therm}$ join smoothly and vanish as $\Lambda \to \infty$, and they differ significantly only in the region $0.5 \leqslant \Lambda \leqslant 4$.

The associated radii $R_\gamma$ decrease as $\Lambda$ increases for all bulk vapour densities; their values reflect the extent of the corresponding drops. The radii $R_s$ for $\rho_{vs} = 0.075$ and 0.1

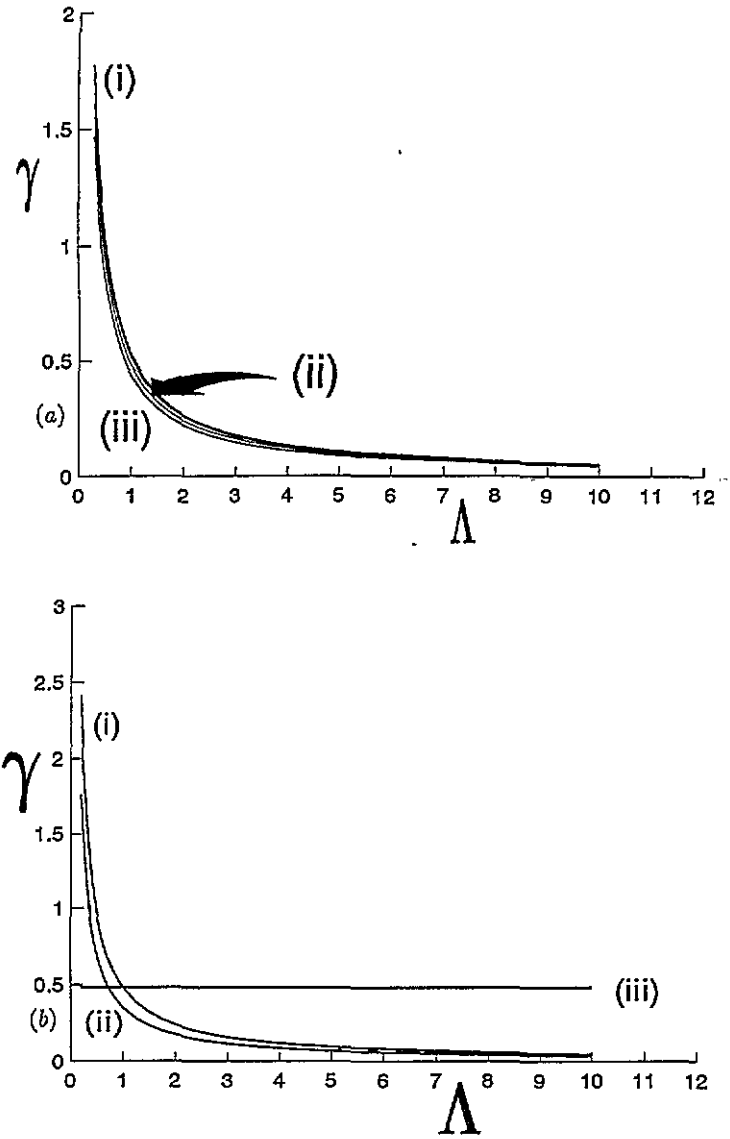


**Figure 8.** (*a*) Surface tension $\gamma_s$ versus $\Lambda$ labelled by the bulk vapour density $\rho_{vs}$: (i) 0.075, (ii) 0.05, between them is that for $\rho_{vs} = 0.1$, (iii) $\gamma_{flat}$ ($\rho_{vc} = 0.041\,478\,49$). (*b*) Surface tensions versus $\Lambda$ for $\rho_{vs} = 0.05$ according to (i) mechanical route, (ii) thermodynamic route, (iii) $\gamma_c$.

(large supersaturation) are nearly identical; they differ considerably with $R_s$ for $\rho_{vs} = 0.05$ but, ultimately, they all join smoothly for $\Lambda > 10$, tending to zero as $\Lambda \to \infty$ (figure 9(*a*)). The other radii ($R_{therm}$, $R_e$) display a similar behaviour, as well. In figure 9(*b*) we plotted $R_s$, $R_{therm}$, $R_e$ for $\rho_{vs} = 0.05$; $R_s$ and $R_e$ practically coincide (this does not imply that Tolman's length $\delta = R_e - R_s$ vanishes), differ from $R_{therm}$ in the interval $0.5 < \Lambda < 6$, and they join smoothly at about $\Lambda \simeq 10$, tending to zero as $\Lambda \to \infty$. These radii behave similarly for the other two bulk vapour densities.

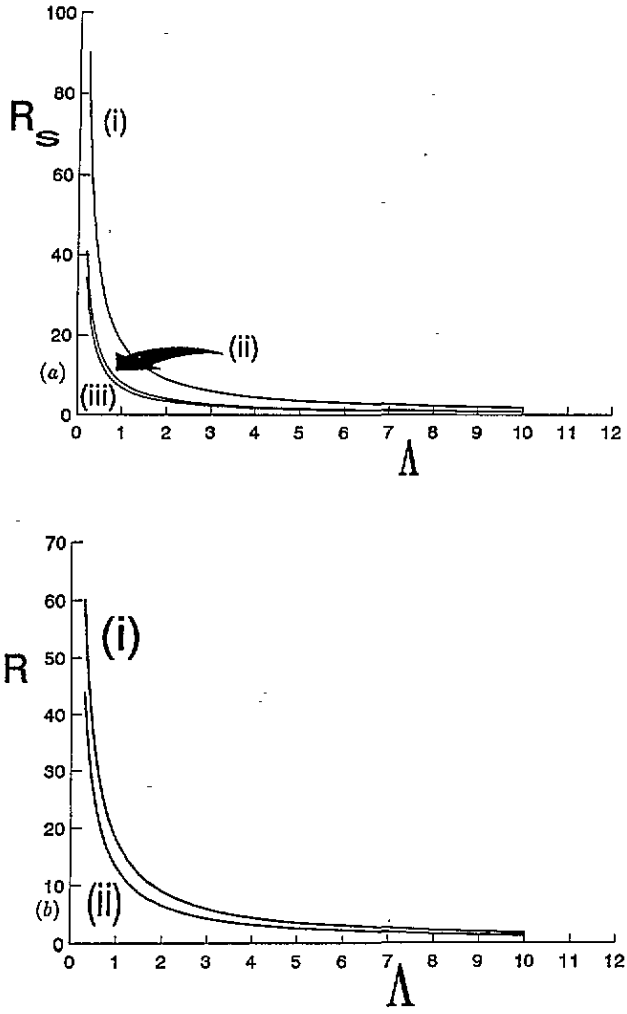


**Figure 9.** (*a*) Radius $R_s$ of the surface of tension versus $\Lambda$ according to the mechanical route (2.32*a*) for various $\rho_{vs}$: (i) 0.05, (ii) 0.075, (iii) 0.1. (*b*) Radii versus $\Lambda$ for $\rho_{vs} = 0.05$: (i) $R_s$ and $R_e$, (ii) $R_{therm}$.

## 4. Discussion

The repulsive forces play a primary role in the structure of most fluids far away from the critical region. However, the slowly varying attractive forces affect the structure in an indirect way, in that the form of the density profile, as a function of $\Lambda$, is left unchanged in comparison with the case $\Lambda = 1$, except that it is either shrunk ($\Lambda > 1$) or spread ($\Lambda < 1$) to accommodate inside the drop the available number of particles of the interior phase for each $\Lambda$.

A necessary prerequisite of bulk thermodynamics is that a large drop encompasses a homogeneous bulk phase so that Lacplace's equation (2.32*b*) is valid. However, this condition is valid only in the case of small supersaturation. The volume of the drop cannot affect the distribution of matter in its interior. $\Lambda$ (attractive forces) determines the radius $R_T^*$ of the drop while the distribution of particles of the interior phase is determined by the

bulk vapour density $\rho_{vs}$ (i.e. hard-sphere repulsions). Thus a large drop $R_T^* = 50$, or even a very large one $R_T^* = 1500$, encompasses a homogeneous phase for $\rho_{vs} = 0.05$ but it does not for $\rho_{vs} = 0.1$. This distinct influence of repulsions and attractions on the system is also reflected in the profiles of the principal tensors.

Both tensions $\gamma_s$ and $\gamma_{therm}$ decrease on increasing $\Lambda$ (or equivalently, on decreasing the corresponding radii $R_s$ and $R_{therm}$) since the drop diminishes as $\Lambda \to \infty$. The tensions $\gamma_s$ for $\rho_{vs} = 0.05$, 0.075 and 0.1 and $\gamma_{flat}$, as functions of $\Lambda$, coincide for $\Lambda < 0.4$ and $\Lambda > 5$ (that is, for smaller and larger drops in comparison with those for $\Lambda = 1$). Thus, it is sensible to use $\gamma_{flat}$ in place of $\gamma_s$ for this range of $\Lambda$ values. An interesting result is that $\gamma_e$, on the one hand, is constant as a function of $\Lambda$ and, on the other, exhibits a distinctly different behaviour in comparison with $\gamma_s$ and $\gamma_{therm}$ although their corresponding dividing surfaces are very close to each other. This peculiar behaviour of $\gamma_e$ is due to the way the equimolar dividing surface is defined through the surface excess density, which is

$$\Gamma(R_\gamma) = \frac{1}{R_\gamma^2}\left(\int_0^{R_\gamma} [\rho(r) - \rho_{Ls}]r^2\,dr + \int_{R_\gamma}^{\infty} [\rho(r) - \rho_{vs}]r^2\,dr\right) \tag{4.1}$$

where $R_\gamma$ is the radius of the dividing surface. The equimolar dividing surface is determined by the condition $\Gamma(R_e) = 0$. As a result of this requirement, the equimolar interface contains an equal number of particles on either side, i.e.

$$\int_0^{R_e} [\rho_{Ls} - \rho(r)]r^2\,dr = \int_{R_e}^{\infty} [\rho(r) - \rho_{vs}]r^2\,dr. \tag{4.2}$$

So there are no excess particles in the interface under consideration for any $\Lambda$, which would change the value of $\gamma_e$ as a function of $\Lambda$. Thus $\gamma_e$ remains constant and is determined solely by the bulk vapour density which, in turn, is determined by the repulsive (hard-sphere) forces. However, whatever finite value any of the surface tensions assumes, the work of formation of a drop

$$W = (4\pi/3)R^2\gamma \tag{4.3}$$

ultimately vanishes as $R \to 0$.

## Acknowledgments

The author expresses his gratitude to Professor G J Papadopoulos and Dr S Messoloras for reading the manuscript.

## References

[1] Sullivan D E 1979 *Phys. Rev.* B 20 3991; 1981 *J. Chem. Phys.* 74 2604
[2] Tarazona P and Evans R 1983 *Mol. Phys.* 48 799
Tarazona P, Telo da Gama M M and Evans R 1983 *Mol. Phys.* 49 283
[3] Teletzke G F, Scriven L E and Davis H T 1982 *J. Chem. Phys.* 77 5794; 1983 *J. Chem. Phys.* 78 1431
[4] Dietrich S and Schick M 1986 *Phys. Rev.* B 33 4952
Pandit R and Wortis M 1982 *Phys. Rev.* B 25 3226
[5] Telo da Gama M M and Evans R 1983 *Mol. Phys.* 48 687
Hadjiagapiou I and Evans R 1985 *Mol. Phys.* 54 383
[6] Hadjiagapiou I 1994 *J. Phys.: Condens. Matter* 6 5305
[7] Rowlinson J S and Widom B 1982 *Molecular Theory of Capillarity* (Oxford: Clarendon)
[8] Evans R 1990 *Liquids at Interfaces (Les Houches Session XLVIII)* ed J F Joanny and J Zin-Justin (Amsterdam: Elsevier) ch 1; 1992 *Fundamentals of Inhomogeneous Fluids* ed D Henderson (New York: Dekker) ch 3